Adaptive Pulse Width Control of Structurally Flexible Systems

Project Description

1. Motivation

The performance of manufacturing machines of all sorts depends upon precise control of the position of some sort of end-effector. Mechanical friction has forever been the thorn in the side of the developers of these machines [1,4]. Consider the simplest of all possible cases, the problem of controlling the position of the rigid-body plant shown in Figure 1. Except when the mass m and the stiction and Coulomb friction levels are known exactly, feedforward plus proportional-derivative feedback control of the position of the mass, y, even when y is measured exactly, results in a steady-state position error. This error occurs when the stiction sticks the plant at a position close enough to the desired position that the proportional gain of the controller multiplied by the position error is not large enough to overcome the stiction force. This error can be reduced by increasing the proportional feedback gain, but, in an application to a physical plant with flexible-body dynamics, the requirement for closed-loop stability places an upper bound on the value of this gain [7,19].

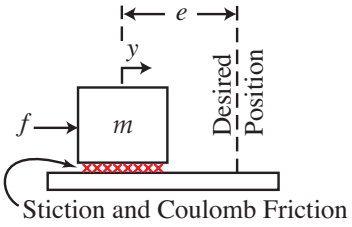

Figure 1. Standard Rigid Body (SRB) plant.

With integral control action added to the feedback controller the gain on the position error is infinite at zero frequency. One might expect that this would eliminate the steady-state position error, but it is well-known that it instead results in a position error limit cycle [1,10].

A 1988 publication by Yang and Tomizuka [20] describes a remarkably effective algorithm for point-to-point position control of rigid-body plants that are subject to mechanical friction, including stiction. This Pulse Width Control (PWC) algorithm is applied only when the plant is close enough to its desired position that stiction forces come into play. When stiction sticks the plant, the algorithm applies a series of fixed-height rectangular force pulses in a feedback fashion to move the plant to its desired position.

The key ideas behind the development of Yang and Tomizuka's algorithm [20] are (1) the use of the simplest possible model that captures the essence of the plant dynamics and (2) the use of a control law that provides high-gain feedback on the position error. Indeed, with the height of the force pulses fixed, the feedback gain on the position error goes to infinity as the position error goes to zero. It is a basic principle of feedback that, under these circumstances, even when the plant parameters are not known exactly, provided the closed-loop system is stable, zero steady-state position error is guaranteed. Consequently, for point-to-point position control of an approximately rigid-body plant, Yang and Tomizuka's PWC algorithm guarantees limit-cycle-free operation and zero steady-state position error, even when the plant parameters, including the stiction and Coulomb friction levels, are not known exactly.

To improve its effectiveness for applications to physical plants, Yang and Tomizuka developed an adaptive version of their PWC algorithm [20]. To demonstrate that the resulting adaptive PWC algorithm was applicable to physical plants, they applied it to point-to-point control of the position of the end-effector of an x-y table [20]. As expected, the result was limit-cycle free operation with the steady-state end-effector position error at the level of the end-effector position measurement error.

2. Objective

In the light of the demonstrated effectiveness of Yang and Tomizuka's adaptive PWC algorithm applied to rigid-body plants, the Principle Investigators for the project proposed here have investigated PWC applied to flexible-body plants.They have shown that the application of Yang and Tomizuka's PWC algorithm to a flexible-body plant can result in a position-error limit cycle. They have furthermore shown that this limit cycle can be avoided, and zero steady-state position error can be achieved, by use of a piecewise-linear-gain PWC law. The project proposed here seeks to take these results to the next level, i.e., to a state of maturity sufficient to attract industrial partners to a subsequent industrially-funded project that will see adaptive PWC with piecewise-linear-gain PWC laws applied to industrial robots and machine tools in bona fide industrial settings.

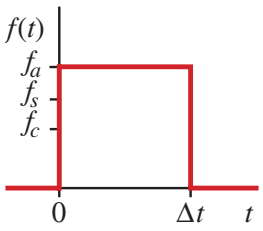

1. $k = 0$.
2. Measure the current position error e_k.
3. Calculate the width
$$\Delta t_k = H_c(e_k)$$
of a force pulse to eliminate e_k.
4. Apply the force pulse from Step 3.
5. Wait until the plant comes to rest.
6. $k = k + 1$.
7. Go to Step 2.

Figure 2. Pulse Width Control (PWC) algorithm.

3. Background

Yang and Tomizuka's PWC algorithm is shown in Figure 2. When the position error is small enough that stiction sticks the plant, the counter k is set to zero, the current position error e_k is measured (see Figure 1), and the PWC law

$$\Delta t_k = H_c(e_k) \tag{1}$$

determines the "width" Δt_k of the kth force pulse. The magnitude of Δt_k specifies the duration of the pulse. The sign of Δt_k specifies the direction of the force. If $\Delta t_k > 0$ the force is applied in the positive y direction (see Figure 1). If $\Delta t_k < 0$ it is applied in the negative y direction. The height (force) of the force pulse is fixed at a value f_a that is larger than both the maximum magnitude of the stiction force f_s and the magnitude of the Coulomb friction force f_c[1]. The force pulse is then applied, and if a position error remains when the plant comes to rest again, the counter k is incremented and the cycle is repeated until the position error is eliminated.

With the change in the steady-state y position of the plant in response to the kth force pulse defined to be

$$\Delta y_k = H_p^{-1}(\Delta t_k) \tag{2}$$

the y position error dynamics of the plant under PWC satisfy

$$e_{k+1} = e_k - H_p^{-1}[H_c(e_k)] \tag{3}$$

The plant model that Yang and Tomizuka used to develop their PWC algorithm (non-adaptive and adaptive forms) [20] is the SRB plant model in Figure 1. For the SRB plant

$$H_p^{-1}(\Delta t_k) = \frac{f_a(f_a - f_c)}{2 f_c m} \Delta t_k^2 \operatorname{sgn}(\Delta t_k) \tag{4}$$

So for the SRB plant the PWC law

$$\Delta t_k = H_c(e_k) = H_p(e_k) = \sqrt{\frac{2 f_c m}{f_a(f_a - f_c)}} \sqrt{|e_k|} \operatorname{sgn}(e_k) \tag{5}$$

will (theoretically) eliminate the y position error in one step.

When the PWC algorithm in Figure 2 and PWC law in (5) are applied to a SRB plant with the mass m, the maximum stiction force f_s, and the Coulomb friction force f_c all known only approximately, under mild assumptions regarding the steady-state position response of the plant to a rectangular force pulse, and with the actual position of the plant measured exactly, limit-cycle-free operation and zero steady-state position error are guaranteed [20].

We applied the PWC algorithm in Figure 2 and PWC law in (5) to control the y position of the end-effector of the industrial robot shown in Figure 3. To obtain the necessary real-time measurements of the position of the end-effector, we used the laser tracker sensor that is also shown in Figure 3 [2,3,15,16,17]. To determine the values for m, f_c, and f_a in (5), we experimentally identified the corresponding values for a SRB plant model of the y-position dynamics of the end-effector of the industrial robot [17]. For the force pulse magnitude f_a we used $f_a = 9 f_s / 8$. The resulting response of the end-effector to a slew command is shown in Figure 4.

---

1. We assume here, without loss of generality, that all stiction and friction forces act "symmetrically" so that, for example, only the sign of the Coulomb friction force changes when the direction of the relative motion between the two contacting surfaces changes.

Figure 3. Industrial robot and laser tracker position sensor.

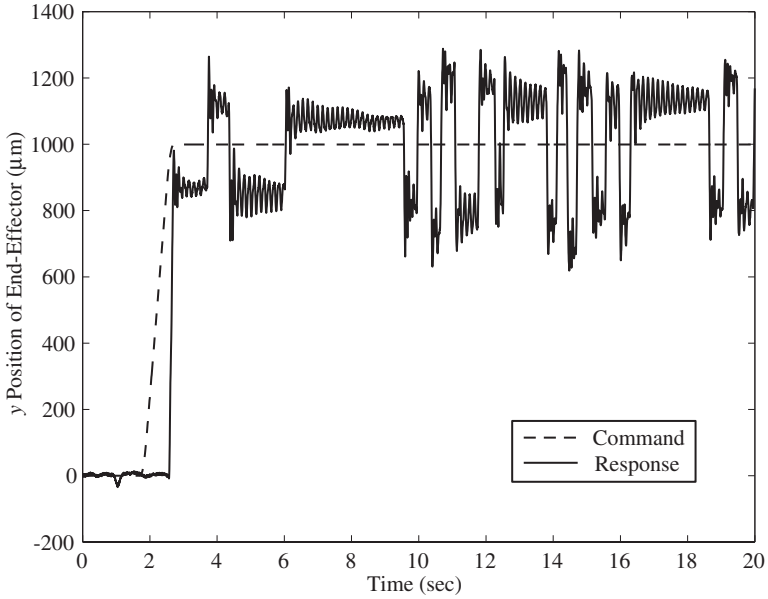

Figure 4. *y* position response under PWC of the end-effector of the industrial robot to a *y* position slew command.

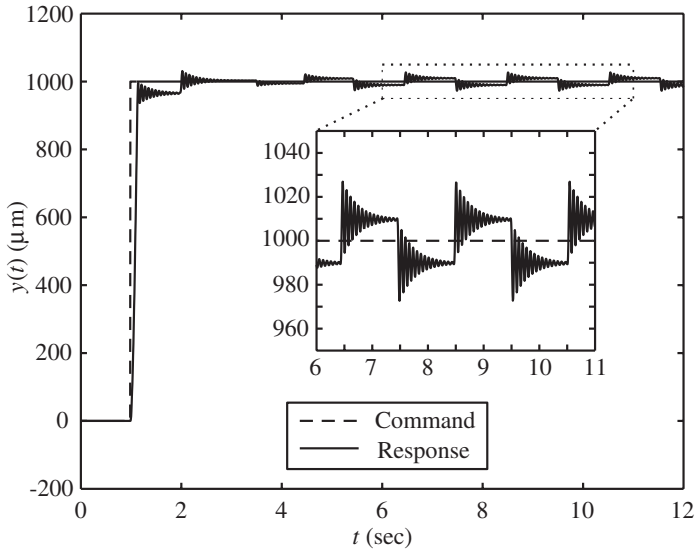

Figure 5. y position response under PWC of the SFB plant equivalent to the *y* position dynamics of the end-effector of the industrial robot to a y position step command.

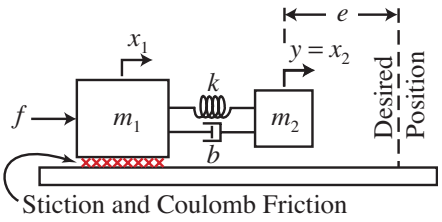

Figure 6. Standard Flexible Body (SFB) plant.

The response in Figure 4 includes a noise-corrupted limit cycle. Thus, Yang and Tomizuka's PWC algorithm applied to a plant having flexible-body dynamics can result in a position error limit cycle. The source of this limit cycle can be determined using a model of the *y* position dynamics of the end-effector of the industrial robot that includes flexible-body dynamics. The response in Figure 5 is the noise-free simulation equivalent to that in Figure 4 obtained using a Standard Flexible Body (SFB) model of the *y* position dynamics of the end-effector of the industrial robot. The structure of this model is shown in Figure 6. We experimentally identified its parameters to make its *y* position dynamics match the *y* position dynamics of the end-effector of the industrial robot [17]. A limit cycle is evident in Figure 5.

The response in Figure 5 duplicates (approximately) the limit cycle behavior in Figure 4. But it does not explain the fundamental cause of the limit cycle in either Figure 4 or Figure 5. Figure 7 is useful in this regard. Figure 7 plots an *upper* bound $H_L^{-1}(\Delta t)$ and a *lower* bound $H_U^{-1}(\Delta t)$ on the steady-state *y* position response, $H_p^{-1}(\Delta t)$, to an applied force pulse of the same SFB plant model as was used to obtain Figure 5 versus the width, Δt, of the applied force pulse [15,17]. The bounds rather than the actual $H_p^{-1}(\Delta t)$ function are plotted because the dynamics of the SFB plant are too complicated for an exact analytical expression for $H_p^{-1}(\Delta t)$ to be obtained [15,17]. Each dot in the dotted curve in Figure 7 represents the corresponding steady-state *y* position response obtained via a piecewise-linear simulation. The dashed curve in Figure 7 shows the steady-state *y* position response versus the width of the applied force pulse for the corresponding SRB plant, i.e., the Δy dictated by (2) and (5) with $m = m_1 + m_2$.

Most importantly, Figure 7 shows that for force pulses of duration less than approximately 0.015 sec, the steady-state *y* position response of the SFB plant model of the *y* position dynamics of the end-effector of the industrial robot is *guaranteed* to be *more than twice* that of the SRB plant model of the same dynamics. Yang and Tomizuka's PWC law uses the SRB plant model to determine the width of each force pulse. So for sufficiently *small y* position errors, Yang and Tomizuka's PWC law applied to the SFB plant model will generate pulse widths that *increase*, rather than decrease, the *y* position error. And for sufficiently *large y* position errors, Yang and Tomizuka's PWC law applied to the SFB plant model will generate pulse widths that *decrease* the *y* position error. These are precisely the conditions

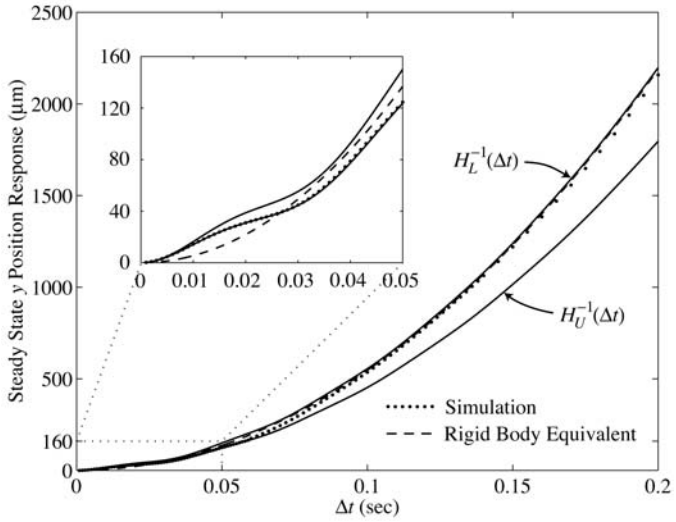

Figure 7. Bounds on the steady-state y position response of the SFB plant equivalent to the y position dynamics of the end-effector of the industrial robot to a force pulse.

that give rise to a limit cycle. Such a limit cycle appears in Figure 5 and also in Figure 4.

The bounds $H_L^{-1}(\Delta t)$ and $H_U^{-1}(\Delta t)$ are derived in [15] and [17]. They can be written as:

$$H_L^{-1}(\Delta t) = \frac{f_a(f_a - f_c)}{2f_c(m_1 + m_2)}\Delta t^2\left[1 + \frac{m_2}{m_1}\frac{1}{(\omega\Delta t)^2}\, r_L(\omega\Delta t)\right] \tag{6}$$

$$H_U^{-1}(\Delta t) = \frac{f_a - f_c}{2(m_1 + m_2)}\Delta t^2\left[1 + \frac{m_2}{m_1}\frac{1}{(\omega\Delta t)^2}\, r_U(\omega\Delta t)\right] \tag{7}$$

with

$$r_L(\omega\Delta t) = 2\frac{f_c}{f_a}\, g(\omega\Delta t) + \frac{f_a - f_c}{f_a}\left[g^2(\omega\Delta t) + \frac{\dot{g}^2(\omega\Delta t)}{\omega^2}\right] \tag{8}$$

$$r_U(\omega\Delta t) = 2g(\omega\Delta t) + \frac{f_a - f_c}{m_2(m_1 + m_2)}\frac{m_1^2}{\left[f_c + \dfrac{2\,m_2(f_a - f_c)}{m_1 + m_2}\right]}\left[(\omega\Delta t)^2 + 2\frac{m_2}{m_1}\omega\Delta t\,\frac{\dot{g}(\omega\Delta t)}{\omega} + \left(\frac{m_2}{m_1}\right)^2\frac{\dot{g}^2(\omega\Delta t)}{\omega^2}\right] \tag{9}$$

$$g(\omega t) = 1 - e^{-\zeta\omega t}\left[\frac{\zeta}{\sqrt{1-\zeta^2}}\sin\left(\sqrt{1-\zeta^2}\,\omega t\right) + \cos\left(\sqrt{1-\zeta^2}\,\omega t\right)\right] \tag{10}$$

$$\zeta = \frac{b}{2\sqrt{k}}\sqrt{\frac{m_1 + m_2}{m_1 m_2}} \qquad\qquad \omega^2 = k\left(\frac{m_1 + m_2}{m_1 m_2}\right) \tag{11}$$

These same bounds can be used to do much more than explain the cause of such limit cycles. It is shown in [15], [16] and [17] that:

1. They can be used to determine sufficient conditions on the SFB plant parameters that guarantee stability and thus limit-cycle-free operation and zero steady-state y position error when Yang and Tomizuka's PWC law in (5) with its nominal gain is applied to a SFB plant.
2. For the case where Yang and Tomizuka's PWC law in (5) with its nominal gain applied to a SFB plant results in a limit cycle, they can be used to determine a factor by which the gain of the PWC law can be reduced to guarantee closed-loop stability and thus limit-cycle-free operation and zero steady-state y position error.

3. For a closed-loop system comprised of a constant-gain or piecewise-linear-gain PWC law applied to a SFB plant, they can be used to determine a value for a performance measure P such that the y position error dynamics is guaranteed to satisfy

$$|e_{k+1}| \leq P\,|e_k| \tag{12}$$

where (provided the closed-loop system is stable)

$$0 \leq P < 1 \tag{13}$$

4. They can be used to determine a piecewise-linear-gain alternative to Yang and Tomizuka's (constant-gain) PWC law. For the case where Yang and Tomizuka's PWC law in (5) with its nominal gain applied to a SFB plant results in a limit cycle, this piecewise-linear-gain PWC law uses low gain when the position error is small to avoid the limit cycle and the nominal gain of Yang and Tomizuka's PWC law when the position error is large to achieve good performance.

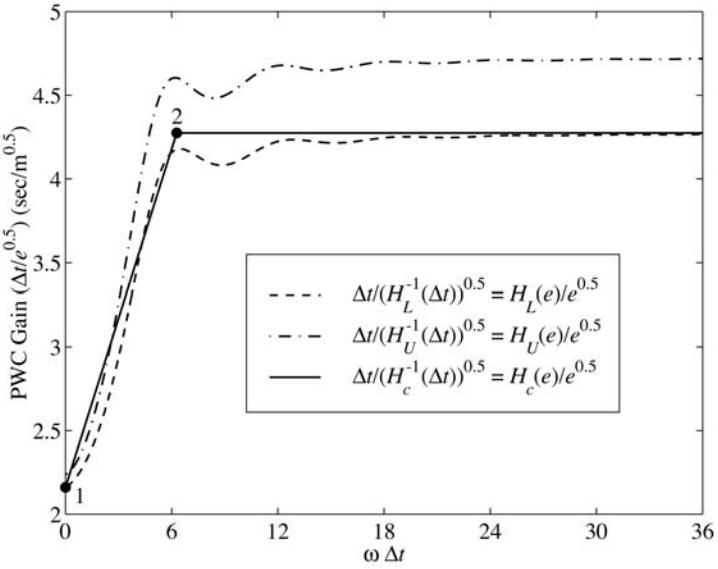

Figure 8. Piecewise-linear PWC gain function to approximate that of the SFB plant equivalent to the y position dynamics of the end-effector of the industrial robot.

This piecewise-linear-gain alternative to Yang and Tomizuka's (constant-gain) PWC law, for the same SFB plant model of the y position dynamics of the end-effector of the industrial robot as was used to obtain Figure 5, is shown in Figure 8 [16,17]. The dot-dashed and dashed curves in Figure 8 are the above-mentioned upper bound $H_U(e)$ and lower bound $H_L(e)$ on the corresponding gain function $H_p(e)$ for this SFB plant. The division by $\sqrt{e}$ in the vertical axis coordinate in Figure 8 is consistent with Yang and Tomizuka's PWC gain function (in (5)) being proportional to $\sqrt{e}$. If Yang and Tomizuka's PWC gain function was plotted in Figure 8, it would appear as a horizontal line through the horizontal portion of the solid curve in Figure 8. To simplify the determination of the coordinates of the points labeled 1 and 2 in Figure 8, which in turn simplifies the determination of an analytic expression for the solid curve in Figure 8, the horizontal axis coordinate in Figure 8 is the width of the applied force pulse, Δt, multiplied by the frequency ω in (11) rather than simply the position error e. See [16] or [17] for details.

The key ideas to be taken from Figure 8 are:

1. The piecewise-linear PWC gain function in Figure 8 does a much better job of matching the corresponding gain function $H_p(e)$ of the SFB plant than does Yang and Tomizuka's PWC gain function for short duration force pulses.
2. The piecewise-linear PWC gain function in Figure 8 exactly matches Yang and Tomizuka's PWC gain function for long duration force pulses.

It is shown in [16] and [17] that the piecewise-linear PWC gain function in Figure 8 can be written in the form of a PWC law as

$$\Delta t_k = H_c(e_k) = \begin{cases} \dfrac{a_0\sqrt{|e_k|}}{1-\dfrac{(a_1-a_0)}{t_0}\sqrt{|e_k|}}\ \mathrm{sgn}(e_k) & 0 \le |e_k| < \left(\dfrac{t_0}{a_1}\right)^2 \\ a_1\sqrt{|e_k|}\ \mathrm{sgn}(e_k) & \left(\dfrac{t_0}{a_1}\right)^2 \le |e_k| \end{cases} \tag{14}$$

with

$$a_0 = \sqrt{\frac{2f_c m_1}{f_a(f_a - f_c)}} \qquad a_1 = \sqrt{\frac{2f_c(m_1+m_2)}{f_a(f_a-f_c)}} \qquad t_0 = \frac{2\pi}{\omega} \tag{15}$$

Recall that Figures 4 and 5 show the actual and simulated closed-loop *y* position response of the end-effector of the industrial robot in Figure 3, obtained the PWC algorithm in Figure 2 and the constant-gain PWC law in (5), to a 1000 micrometer slew command. When the piecewise-linear-gain PWC law in (14) is used instead of the constant-gain PWC law in (5), the corresponding responses are shown in Figures 9 and 10 [2,3,16,17]. Most importantly, in Figure 9 the actual *y* position response of the end-effector of the industrial robot includes no limit cycle and settles to within the tens of micrometers accuracy of the laser tracker measurements of the position of the end-effector.

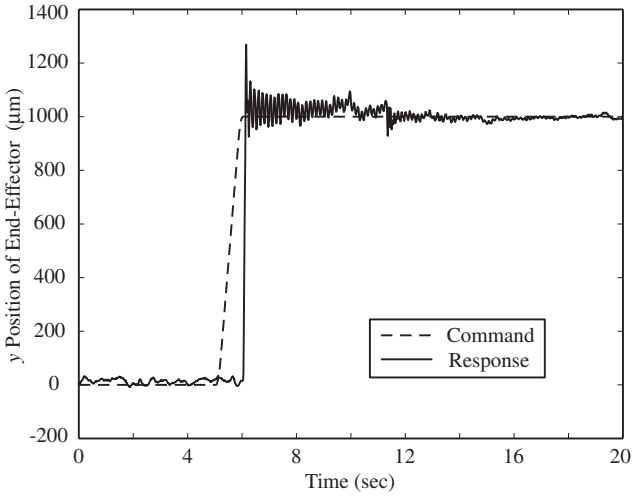

Figure 9. *y* position response of the end-effector of the industrial robot to a *y* position slew command obtained using the piecewise-linear-gain PWC law.

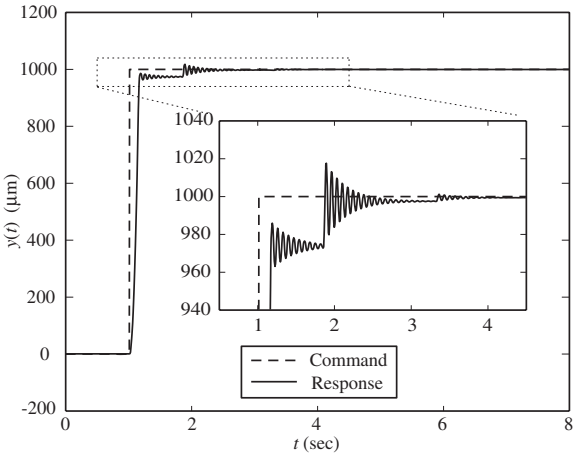

Figure 10. y position response under PWC of the SFB plant equivalent to the *y* position dynamics of the end-effector of the industrial robot to a y position step command obtained using the piecewise-linear-gain PWC law.

4. Project Plan

The major points of Section 3 can be summarized as follows:

1. For point-to-point position control of a rigid-body plant subject to mechanical friction, including stiction, even when the plant parameters are not known exactly, the combination of the PWC algorithm in Figure 2 and the PWC law in (5) guarantees limit-cycle-free operation and zero steady-state position error.
2. The plant dynamics model that Yang and Tomizuka utilized to develop their PWC law in (5) is the SRB plant model in Figure 1.
3. To improve its effectiveness for applications to physical plants, Yang and Tomizuka developed an adaptive version of the PWC algorithm in Figure 2.

The authors of this proposal have utilized the SFB plant model in Figure 6 to:

4. Show that the combination of the PWC algorithm in Figure 2 and the PWC law in (5), when applied to a flexible-body plant under the otherwise identical circumstances, can result in a position error limit cycle.
5. Explain the occurrence of the position error limit cycle that can occur when the combination of the PWC algorithm in Figure 2 and the PWC law in (5) is applied to a flexible-body plant.
6. Determine a reduction in the gain of the PWC law in (5) that is guaranteed to eliminate the limit cycle and achieve zero steady-state position error, when the combination of the PWC algorithm in Figure 2 and the PWC law in (5) applied to a SFB plant results in a position error limit cycle.
7. Determine a piecewise-linear-gain alternative to the PWC law in (5). The former utilizes lower gain compared to the constant-gain PWC law in (5) when the position error is small and the same gain as the constant-gain PWC law in (5) when the position error is large. The lower gain for small position errors eliminates the limit cycle that occurs when the constant-gain PWC law in (5) is applied to some flexible-body plants. The same gain as the constant-gain PWC law in (5) for large position errors guarantees the same performance (the same rate of convergence of the position error toward zero) as the constant-gain PWC law in (5) when the position error is large.

And lastly, the authors of this proposal have:

8. Demonstrated each of the above points 4, 6 and 7 in applications to point-to-point control of the position of the end-effector of the industrial robot shown in Figure 3.

We believe that the results referred to in items 4 – 8 above constitute a proof of concept that a PWC algorithm that both (1) utilizes a piecewise linear gain PWC law and (2) adapts its parameters to changes in the physical plant being controlled will make possible, in those many situations in which mechanical friction, and, in particular stiction, has proven to be a significant issue, dramatic improvements in the accuracy to which point-to-point control of the position of an end-effector (e.g., for an industrial robot or a machine tool) can be achieved. The project proposed here seeks to take this proof of concept to the next level, i.e., to a state of maturity sufficient to attract industrial partners to a subsequent industrially-funded project that will see adaptive PWC with piecewise-linear PWC laws applied to industrial robots and machine tools in bona fide industrial settings.

A unique team of researchers will be assembled in this project to meet this goal. Martin Berg, the PI from the University of Washington, completed his PhD at Stanford University under J. David Powell (see, e.g., [5] and [6]). Professor Berg has been teaching and conducting research in control system design at the University of Washington since 1986. Keith Buffinton, the PI from the Bucknell University, completed his PhD at Stanford University under Thomas Kane (see, e.g., [8] and [9]). Professor Buffinton has been teaching and conducting research in dynamic system modeling and analysis at Bucknell University since 1988. The publications recently co-authored by Professors Berg and Buffinton [2,3,11,15,16] attest to the value that the dovetailing of their expertise in controls and dynamics, respectively, will contribute to this project.

The additional team members will include one University of Washington graduate student who will focus, under the advisorship of Professors Berg and Buffinton, on the development of mechanisms to make a PWC algorithm that utilizes a piecewise-linear-gain PWC law adapt its parameters to changes in the parameters of the physical plant being controlled. Bucknell University graduate students, also under the joint advisorship of Professors Berg and Buffinton, will focus on the largely uncharted territory of PWC applied to plants having multiple dynamically coupled axes. And last but not least, undergraduate students at the University of Washington and at Bucknell University will have significant roles in the project, to tackle the smaller scale issues that our experience suggests invariably arise when PWC is applied to physical systems.

The following two subsections below discuss the two greatest challenges to be undertaken in this project, namely (1) the development of mechanisms to make a PWC algorithm that utilizes a piecewise-linear-gain PWC law adapt its parameters to changes in the physical plant being controlled, and (2) the development of modifications to the classical PWC strategy to accommodate physical plants that utilize multiple dynamically coupled axes.

4.1 Adaptation

The rate of convergence of the position error to zero under PWC is what we refer to as the performance of a PWC system. This performance directly depends upon the accuracy to which the PWC law determines the pulse width Δt_k to eliminate the current position error e_k. The end-effector position dynamics of industrial robots and machine tools (e.g., the end-effector position vibration frequencies) depend highly upon factors such as the position and orientation of the end-effector within the workspace of the device and the temperature in the vicinity of the device. It follows that, to achieve high performance in an application of PWC to an industrial robot or a machine tool, the PWC law *must* adapt its parameters to changes in the end-effector position dynamics of the physical plant being controlled.

Yang and Tomizuka's PWC law in (5) can be written as

$$\frac{\Delta t_k}{\sqrt{|e_k|}\,\mathrm{sgn}(e_k)} = h_0(\Delta t_k)\, a_0 \tag{16}$$

with

$$h_0(\Delta t_k) = 1 \qquad a_0 = \sqrt{\frac{2 f_c m}{f_a(f_a - f_c)}} \tag{17}$$

During each cycle through the PWC algorithm (in Figure 2), the duration, Δt_k, of the force pulse to be applied is calculated, the force pulse is applied, and the resulting change in the steady-state y-position of the plant, Δy_k, is measured. If the dynamics of the physical plant being controlled were exactly represented by the dynamics of a SRB plant (in Figure 1), with the mass of the plant, m, and the Coulomb friction force that acts on the plant, f_c, known exactly, then, during each cycle through the PWC algorithm, this equation (for the $\Delta t_k > 0$ case)

$$\frac{\Delta t_k}{\sqrt{\Delta y_k}} = h_0(\Delta t_k)\, a_0 \tag{18}$$

would be satisfied exactly.

In practice, the dynamics of the physical plant being controlled are never exactly represented by the dynamics of a SRB plant, and, even to the extent that they are, the mass of the plant, m, and the Coulomb friction force that acts on the plant, f_c, are never known exactly. On the other hand, that a new Δy_k value is measured that corresponds to a new known Δt_k value during each pass through the PWC algorithm, together with the fact that the single parameter, a_0, in the PWC law in (5) is linearly related to $\Delta t_k / \sqrt{\Delta y_k}$ via (18) implies that a recursive least squares algorithm could be used to update the single parameter, a_0, in the PWC law in (5) during each pass through the PWC algorithm. Yang and Tomizuka's adaptive PWC algorithm (self-tuning regulator and model reference adaptive control versions) is the combination of the PWC algorithm in Figure 2 and such a recursive least squares algorithms that adapts the single parameter, a_0, of the PWC law in (5) to changes in the end-effector position dynamics of the physical plant being controlled [20].

For the piecewise-linear-gain PWC law in (14), it is straightforward to show that the dual to (18) (again for the $\Delta t_k > 0$ case) is

$$\frac{\Delta t_k}{\sqrt{\Delta y_k}} = h_0(t_0, \Delta t_k)\, a_0 + h_1(t_0, \Delta t_k)\, a_1 \tag{19}$$

with

$$h_0(t_0, \Delta t_k) = \begin{cases} 1 - \dfrac{\Delta t_k}{t_0} & 0 < \Delta t_k \le t_0 \\ 0 & t_0 < \Delta t_k \end{cases} \qquad h_1(t_0, \Delta t_k) = \begin{cases} \dfrac{\Delta t_k}{t_0} & 0 < \Delta t_k \le t_0 \\ 1 & t_0 < \Delta t_k \end{cases} \tag{20}$$

Thus, for a PWC algorithm that utilizes the piecewise-linear-gain PWC law in (14), that a new Δy_k value is measured

that corresponds to a new known Δt_k value during each pass through the PWC algorithm, together with the fact that the two parameters a_0 and a_1 in the piecewise-linear-gain PWC law in (14) are linearly related to $\Delta t_k / \sqrt{\Delta y_k}$ via (19) implies that, given a value for t_0, a recursive least squares algorithm could be used to update the two parameters a_0 and a_1 in the piecewise-linear-gain PWC law in (14) during each pass through the PWC algorithm.

In keeping with Yang and Tomizuka's approach, the starting point, in the project proposed here, in our efforts to make a PWC algorithm that utilizes a piecewise-linear-gain PWC law adapt to changes in the physical plant being controlled will be just such a recursive least squares algorithm, i.e., a recursive least squares algorithm to update the parameters a_0 and a_1 in the piecewise-linear-gain PWC law in (14) during each pass through the PWC algorithm. This, however, will be only the starting point. It will be only the starting point because such an algorithm will do nothing to update the parameter t_0 in the piecewise-linear-gain PWC law in (14). And it is this parameter t_0 that defines the location of the "knee" in the piecewise-linear gain function in Figure 8.

Moreover, in keeping with the objective of this project, i.e., to move PWC with piecewise-linear-gain PWC laws to a state of maturity sufficient to attract industrial partners to a subsequent industrially-funded project that will see PWC with piecewise-linear-gain PWC laws applied to industrial robots and machine tools, a comprehensive effort will be undertaken, in the project proposed here, to adapt *all* parameters of a PWC algorithm that utilizes a piecewise-linear-gain PWC law, including *all* parameters of the piecewise-linear-gain PWC law *and* the height of the forces pulses that the PWC algorithm applies to the physical plant being controlled, to changes in the end-effector position dynamics of the physical plant being controlled.

4.2 Pulse Width Control of Multiple Dynamically Coupled Axes

Pulse width control, as it is described in Section 3, is applicable to devices having multiple dynamically coupled axes provided the dynamic coupling between the axes is sufficiently small. The application of Yang and Tomizuka's adaptive PWC algorithm to an x-y table that is referred to in Section 1 is one case in point. The application of piecewise-linear-gain PWC laws to the x, y and z axes of the six-axis industrial robot in Figure 3 is another. The majority of industrial robots and machine tools in use today, however, are required to execute maneuvers that require the coordinated motion of several dynamically coupled axes. To date, no investigation of the application of PWC to such devices has been reported.

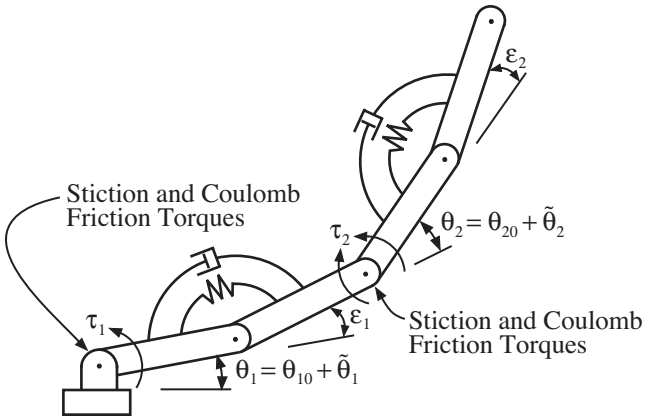

Figure 11. Flexible-body plant with two dynamically coupled axes.

The development of modifications to the classical PWC strategy to accommodate physical plants having multiple dynamically coupled axes will be a principal topic of the project proposed here. Consider the planar two-axis robotic arm shown in Figure 11. A pin joint at the mid point of each link and a rotational spring and a rotational damper that act about the axis of each such pin joint model flexibility in the two links. Stiction and Coulomb friction torques arise at each of the two actuated axes (due, e.g., to actuator gearing).

The flexible-body plant in Figure 11 is the two-axis rotational equivalent to the SFB plant in Figure 6. Most notably, the two axes of the former are dynamically coupled and the strength of this coupling is a function of the elbow angle θ_2. In the project proposed here, we will develop modifications to the classical PWC strategy that will accommodate such plants. Key to this development will be the understanding that, as discussed in Section 1, PWC is to be applied only when the end-effector of the plant is close enough to its desired position that stiction forces come into play. (For large-scale motions of the end-effector along a path, stiction forces are not an issue and standard, e.g., proportional-derivative, control strategies can be used.) The upshot of this, in practice, is that PWC is to be applied

only to effect small point-to-point displacements of the position of the end-effector. For example, for the six-axis industrial robot shown in Figure 3, the end-effector position displacements for which PWC is appropriate span not more than a few millimeters.

Thus, in order to develop a modified PWC strategy to accommodate the likes of the flexible-body plant in Figure 11, it will be necessary to modify the classical PWC strategy to accommodate the dynamic coupling between the axes, but this development will be greatly simplified by the fact that it need only consider the linear small-perturbation dynamics of the plant, i.e., for small perturbations of the position of the end-effector away from its targeted position.

In the project proposed here, the starting point for our development of modifications to the classical PWC strategy to accommodate physical plants that utilize multiple dynamically coupled axes will be the development of the modification necessary to accommodate the flexible-body plant with two dynamically coupled axes shown in Figure 11.While the dynamic coupling between the two axes of this plant are undoubtedly not representative of the dynamic coupling that exists between all axes of all physical devices to which one might wish to apply PWC, our past experiences with PWC leads us to expect that this starting point will lead us to understandings that will enable us to develop modifications to the classical PWC strategy that will accommodate many important configurations of flexible-body plants that utilize multiple dynamically coupled axes, including many important configurations of industrial robots and machine tools.

4.3 Application to Physical Devices

As stated in the Objective section above, this project seeks to take PWC to the next level, i.e., to a state of maturity sufficient to attract industrial partners to a subsequent industrially-funded project that will see adaptive PWC algorithms that utilize piecewise-linear-gain PWC laws applied to industrial robots and machine tools in bona fide industrial settings. To meet this objective, it is imperative that the methodology for designing adaptive PWC algorithms that utilize piecewise-linear-gain PWC laws to be developed in this project be convincingly demonstrated to be applicable to physical devices. A two-pronged approach will be taken in this project to meet this imperative: (1) the developments of all of the adaptation algorithms that are undertaken in this project will include rigorous proofs of the theoretical stability of the resulting position error dynamics, and (2) the resulting methodology for designing adaptive PWC algorithms that utilize piecewise-linear-gain PWC laws will be convincingly demonstrated via applications to several hardware testbeds. Three of the hardware testbeds that will be used for the latter are described in the following subsections.

4.3.1 Flexible One-Link Robotic Arm

The testbed shown in Figure 12, is located in the Robotics and Control Systems Laboratory on the University of Washington campus. It is a planar flexible-one-link robotic arm [14]. The end-effector of this testbed is mounted on a disk that floats on an air bearing on the horizontal surface of a granite table. The air bearing support provides that the system can be configured with a very flexible link (first bending mode frequency near π rad/sec) to emulate the structural flexibilities that are as important, but much less obvious, in industrial robots and machine tools when point-to-point control of the position of the end-effector to the resolution of the likes of a laser tracker sensor is the objective.

The actuator for this testbed is a direct-drive torque motor with peak torque 0.919 Nm. The amount of squeeze that a bicycle brake applies to a flywheel on the motor shaft can be adjusted to add friction to the actuation path (see Figure 12). And the amount free-play in a coupling mechanism on the motor shaft can be adjusted to add a desired amount backlash to the actuation path.

An encoder with resolution 0.0036 deg measures the joint position on each side of the backlash mechanism. And an overhead infrared-light-based sensor (not shown in Figure 12) measures the position of the end-effector in real-time, delivering 67 measurements/sec, with less than 1/67 sec data latency, to 0.5 mm (rms error) accuracy.

The signal processing system for implementing command and control algorithms for this testbed is a fully open-architecture system that employs a VME backplane, a PowerPC 604 single-board computer, I/O boards, the VxWorks real-time operating system, and the Constellation software package [14].

4.3.2 Flexible Two-Link Robotic Arm

The testbed shown in Figure 13 is also located in the Robotics and Control Systems Laboratory on the University of Washington campus. It is the two-link equivalent of the testbed in Figure 12 without the corresponding mechanical mechanisms for generating friction or backlash in its actuation paths [11]. The elbow and end-effector of this testbed float on air bearings on the same granite table as the testbed in Figure 12. The air bearing supports provide that the

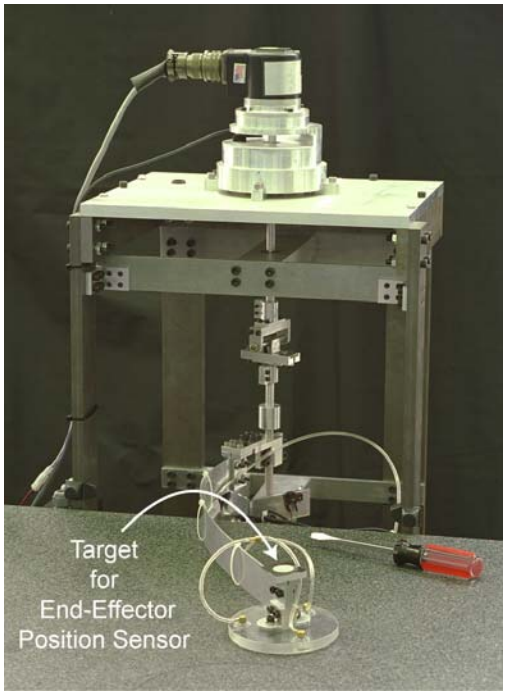

Friction Mechanism

Backlash Mechanism

Figure 12. Flexible one-link robotic arm with friction and backlash in actuation path.

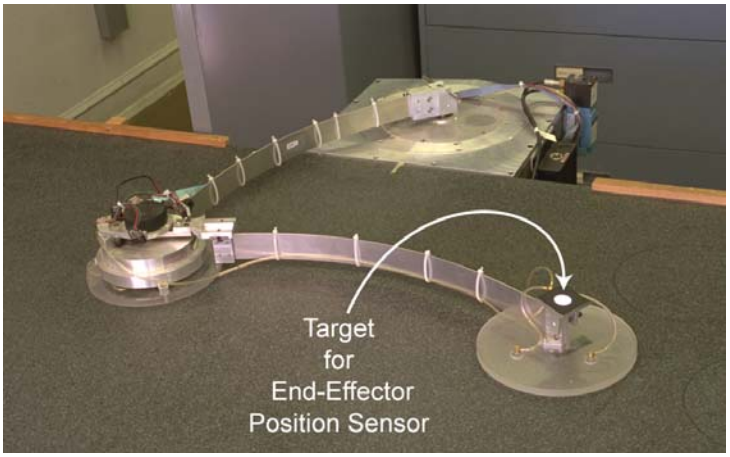

Figure 13. Flexible two-link robotic arm.

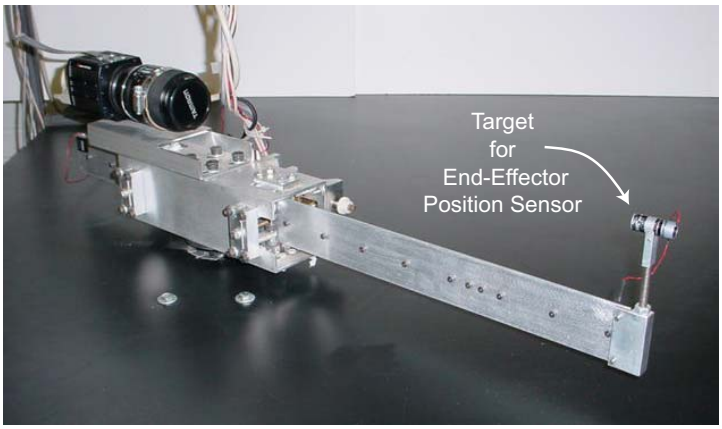

Figure 14. Two-link robotic arm with one revolute joint, one prismatic joint and one flexible link.

system can be configured with very flexible links (first bending mode frequency near π rad/sec). The actuators at the shoulder and elbow joints are direct-drive torque motors with peak torques 2.6 and 0.62 Nm, respectively. Optical encoders, each with resolution 0.0879 degrees, measure the two joint positions. The same infrared-light-based sensor that measures the position of end-effector of the testbed in Figure 12 in real-time measures the position of the end-effector of this testbed in real-time, delivering 67 measurements/sec, with less than 1/67 sec data latency, to 0.5 mm (rms error) accuracy.

The signal processing system for this testbed is the same fully open-architecture VME/PowerPC 604/VxWorks/Constellation system that is used for the testbed in Figure 12. For this project, this system, for this testbed, will have two roles: (1) to implement PWC algorithms to achieve point-to-point control of the position of the end-effector, and (2) to implement, at a much higher sampling rate at each of the two axes, a collocated encoder-to-actuator feedback loop to emulate the stiction, Coulomb, and other friction forces that would occur if geared, rather than direct-drive, motors were used to actuate this testbed's axes.

4.3.3 Two-Link Robotic Arm with Prismatic Joint and Flexible Link

The testbed shown in Figure 14 is located in the Laboratory for Integrated Design, Manufacturing and Robotics at Bucknell University. It is a two-link robotic arm with one revolute joint and one prismatic joint. The translating link is flexible and its effective length varies with its position as it traverses the prismatic joint. When the translating link is fully extended, its first bending frequency is 5.2 Hz. The workspace of the arm is an annular region with an inner radius of 0.188 m and an outer radius of 0.563 m.

The position of the end-effector of the arm is measured relative to the first link by means of a line scan camera with 1024 picture elements. The camera and associated interface board are capable of producing 9,000 measurements per second of end-effector displacement with a resolution of 0.01 mm and a data latency less than 0.1 ms. The positions of the revolute and prismatic joints are measured by optical encoders with resolutions of 0.0015 deg and 0.003 mm, respectively. The software interface has recently been completely upgraded, thus providing a much simpler and more flexible interface in which to performance experiments.

5. Broader Impacts of this Project

In manufacturing today, from micro- and nano-scale work in the electronics industry to the comparatively macro-scale world of the aerospace industry, the expectation is unmistakably that, as time progresses, manufacturing machines will be capable of manufacturing parts to ever more exacting standards. The only hope for meeting this expectation is that manufacturing machines be developed to take advantage of the remarkable rate of innovation that is evident today in two areas, namely computing and instrumentaion [18]. The six-axis industrial robot and laser tracker sensor pictured in Figure 3 are a case in point. The laser tracker is capable of delivering 1000 measurements per second, with data latency 0.001 sec, of the position of a retroreflector to an accuracy in the tens of micrometers. Replacement of the robot's original-equipment signal processing system with a modern one that harnesses up-to-date computing technologies made it possible to incorporate the use of the laser tracker's measurements of the position of a retroreflector on the robot's end-effector into the logic that is used to control the position of the end-effector. As discussed in Section 3 of this proposal, this made it possible to achieve point-to-point control of the position of the end-effector to the tens-of-micrometers accuracy of the laser tracker measurements. This is more than an order-of-magnitude improvement over the point-to-point end-effector position control accuracy that can be achieved with the factory version of this robot.

The material in Section 3 also makes the point that innovations in computing technology and instrumentation alone will not give rise to the manufacturing machines that will meet either the present or the future expectations of our society. We (Professors Berg and Buffinton) are enthusiastic about the opportunities that the project proposed here will provide to a team of researchers, comprised of undergraduate through Phd-level students at Bucknell University and the University of Washington and ourselves, to make what we believe will be a key contribution to the development of manufacturing machines that will meet the present and future expectations of our society. More specifically, we believe that the methodology for the design of adaptive PWC algorithms that will be developed by our research team in this project will ultimately result in dramatic demonstrations of what can be accomplished, with industrial robots and machine tools, in terms of point-to-point control of end-effector position, when recent innovations in instrumentation and computing technologies are effectively utilized.

The broader impacts of this project will be significantly enhanced by the fact that this work will be performed collaboratively by a predominantly undergraduate institution (Bucknell University) and a Research I institution (University of Washington). The basic PWC idea is simple enough that it can be readily understood by undergraduates. Consequently this project will provide a proportionately unusual number of opportunities for

undergraduate students to contribute to the research results that will be obtained. In addition to one MS/PhD student at the University of Washington for three years and two MS students at Bucknell, each for one year, we plan to have six to ten undergraduate students participate directly in the project for shorter periods of time. Bucknell has an established tradition of involving undergraduates in faculty research and this project will continue that tradition. The Bucknell University web page that is dedicated to undergraduate research (with the individual pictured in its upper left corner being Professor Buffinton), at

`www.bucknell.edu/The_Bucknell_Difference/Undergraduate_Research.html`

describes Bucknell's strong emphasis on undergraduate research and its support for students "across all disciplines [to] find opportunities for meaningful scholarly work with professors who want to help them develop their knowledge and ability to think critically." The undergraduate research program at the University of Washington, for which the corresponding web page is at

`www.washington.edu/research/urp`

is a thriving if more recent tradition at the University of Washington. The undergraduate research programs at both universities will be strengthened by the significant roles that undergraduate students will have in this project.

Students at Bucknell and at the University of Washington will work on this project during both the academic year and the summer, providing time and opportunities for significant one-on-one interactions between all research team members (including Professors Berg and Buffinton). Particularly for the undergraduate students, this will promote learning of both content and methods of research and investigation. Studies show that the involvement of undergraduates in faculty research projects significantly enhances the probability that these students will decide to pursue advanced degrees. Furthermore, future engineering faculty are disproportionately educated at predominantly undergraduate institutions, such as Bucknell, where they have the opportunity to work closely with faculty on their research.

This project will also be particularly beneficial to Professor Buffinton in a way that will impact future Bucknell students not directly involved in the project. While Professor Buffinton has conducted research into numerous aspects of the dynamics of robotic mechanisms, the opportunities for him to be involved, at Bucknell, in the sort of controls-related research that will be undertaken in this project are limited. The experience and expertise in this area that he will gain as a result of his role in this project will undoubtedly enhance the content of the Robotics, System Dynamics, Advanced Dynamics, and Systems Modeling course that he teaches at Bucknell.

There will also be significant broader impacts for the students at Bucknell University and the University of Washington who participate in the project that stem from the different natures of the educational environments at two schools. The MS/PhD student at the University of Washington will serve not only as a source of advanced knowledge for the University of Washington and Bucknell undergraduate and Bucknell MS student participants, but also as a role model for the undergraduate and MS participants who may be considering the pursuit of doctoral degrees themselves. Moreover, for the MS/PhD student at the University of Washington, working with and mentoring the University of Washington and Bucknell undergraduate students and the Bucknell MS students will provide opportunities to develop skills that will be crucial should he or she should choose to pursue a faculty position at a future time.

Another broader impact of this project specifically relates to the collaborative relationship that has developed between Professors Berg and Buffinton. Professor Berg and Professor Buffinton have collaborated on a total of six published works that focus on the dynamics and control of structurally flexible systems. Particularly given the relatively small number of faculty in mechanical engineering at Bucknell (9 permanent positions), the opportunities for Professor Buffinton to interact closely and continuously with colleagues working in advanced areas of dynamics and control at Bucknell are limited. With the funding of this proposal, the partnership between Professors Berg and Buffinton, which has been so successful in the past, will continue, to the substantial benefit of the University of Washington and Bucknell University and likewise to the substantial benefit of the technical community with interests in the dynamics and control of structurally flexible systems as a whole.

Dissemination of the results of this project will be achieved in a number of ways. The faculty and students that are directly involved will share the knowledge and results that they obtain with colleagues and also, in the case of the professors, with current and future students. The results will of course also be presented to the profession at conferences and reported in journal publications. Intramural and extramural dissemination of results will also be achieved through the regularly scheduled site visits (Professor Buffinton to the University of Washington and Professor Berg to Bucknell, once per year). These site visits will be scheduled during the academic year with a formal presentation to faculty and students planned for each site visit.

References Cited

[1] Armstrong-Helouvry, B., Dupont, P., and De Witt, C. C., 1994, "A Survey of Models, Analysis Tools and Compensation Methods for the Control of Machines with Friction," *Automatica*, **30**, pp. 1083-1138.

[2] Berg, M. C., Rathbun, D. B., and Buffinton, K. W., 2002, "Precise Control of the Position of the End-Effector of an Industrial Robot," Proceedings of the 2002 ISCIE/ASME Japan-USA Symposium on Flexible Automation.

[3] Berg, M. C., Rathbun, D. B., and Buffinton, K. W., 2002, "Pulse Width Control of the Position of the End-Effector of an Industrial Robot," Proceedings of the 2002 IFAC Conference on Mechatronic Systems.

[4] de Wit, C. C., Noel, P., Aubin, A. and Brogliato, B., 1991, "Adaptive Friction Compensation in Robot Manipulators: Low Velocities," *International Journal of Robotics Research*, **10**, pp. 189-199.

[5] Franklin, G. F., Powell, J. D., and Emami-Naeini, A, 1994, Feedback Control of Dynamic Systems, Addison Wesley, New York.

[6] Franklin, G. F., Powell, J. D., and Workman, M, 1997, Digital Control of Dynamic Systems, Addison Wesley, New York.

[7] Freudenberg, J. S. and Looze, D. P., 1985, "Right Half Plane Poles and Zeros and Design Tradeoffs in Feedback Systems," *IEEE Transactions on Automatic Control*, **30**, pp. 555-565.

[8] Kane, T. R. and Levinson, D., 1985, Dynamics: Theory and Applications, McGraw-Hill, New York.

[9] Kane, T. R., Likins, P. and Levinson, D., 1993, Spacecraft Dynamics, McGraw-Hill, New York.

[10] Khalil, H. K., 2002, Nonlinear Systems, Prentice-Hall, Upper Saddle River, NJ.

[11] Lertpiriyasuwat, V., Berg, M. C., and Buffinton, K. W., 2000, "Extended Kalman Filtering Applied to a Two-Axis Robotic Arm with Flexible Links," *International Journal of Robotics Research*, **19**, pp. 254-270.

[12] Lertpiriyasuwat, V. and Berg, M. C., in review, "Real-Time Adaptive Estimation of End-Effector Position and Orientation for Industrial Robots, Part 1: Algorithm Development," *IEEE/ASME Transactions on Mechatronics*.

[13] Lertpiriyasuwat, V. and Berg, M. C., in review, "Real-Time Adaptive Estimation of End-Effector Position and Orientation for Industrial Robots, Part 2: Experimental Results," *IEEE/ASME Transactions on Mechatronics*.

[14] Mason, G. A., Pongpunwattana, A., and Berg, M. C., 2002, "A Flexible Test Bed for Control System Analysis and Verification," *Mechatronics*, Elsevier Science, Ltd., London, **12**, pp. 891-904.

[15] Rathbun, D. B., Berg, M. C., and Buffinton, K.W., 2004, "Pulse Width Control for Precise Positioning of Structurally Flexible Systems Subject to Stiction and Coulomb Friction," *ASME Journal of Dynamic Systems, Measurement and Control*, **126**, pp. 131-138.

[16] Rathbun, D. B., Berg, M. C., and Buffinton, K.W., 2004, "Piecewise-Linear-Gain Pulse Width Control for Precise Positioning of Structurally Flexible Systems Subject to Stiction and Coulomb Friction," *ASME Journal of Dynamic Systems, Measurement and Control*, **126**, pp. 139-143.

[17] Rathbun, D. B., 2001, "Pulse Modulation Control for Precise Positioning of Structurally Flexible Systems Subject to Stiction and Coulomb Friction," PhD Dissertation, Department of Electrical Engineering, University of Washington, Seattle.

[18] Sharke, P., 2002, "Brawn + Brains > 1: Having Acquired Muscle and Grace, Machine Tools Begin Wising Up," *Mechanical Engineering*, ASME, New York, **124**, pp. 46-49.

[19] Spector, V. A. and Flashner, H., 1990, "Modeling and Design Implications of Noncollocated Control in Flexible Systems," *ASME Journal of Dynamic Systems, Measurement and Control*, **112**, pp. 186-193.

[20] Yang, S. and Tomizuka, M., 1988, "Adaptive Pulse Width Control for Precise Positioning Under the Influence of Stiction and Coulomb Friction," *ASME Journal of Dynamic Systems, Measurement and Control*, **110**, pp. 221-227.